

## The Structure of Pyrazole, $C_3H_4N_2$ , at 295 K and 108 K as determined by X-Ray Diffraction

TROELS LA COUR\* and SVEND ERIK RASMUSSEN

*Department of Inorganic Chemistry, University of Aarhus, DK-8000 Aarhus C, Denmark*

The structure of pyrazole has been re-investigated using X-ray diffractometry and  $MoK\alpha$ -radiation. One set of data was collected at room temperature using a four-circle diffractometer. Another set was collected also at room temperature using an equi-inclination diffractometer. The latter was employed for collecting data at 108 K as well. The three sets of data were refined independently using various constrained and unconstrained models. The refinements show that the atomic vibrations are not approximated well using a model assuming the molecules to move as rigid bodies. The two sets of room temperature data are in stronger disagreement with the rigid body model than the low temperature data. The least squares matrices show that corresponding parameters of the two crystallographically independent molecules are strongly correlated. The geometry of the pyrazole molecule indicates a high degree of de-localized  $\pi$ -bonding.

The crystal structure of pyrazole was determined by Ehrlich<sup>1</sup> in 1960 from photographically recorded X-ray diffraction data of the three pinacoid projections. An X-ray re-determination by Berthou *et al.*<sup>2</sup> and a neutron diffraction study by Larsen *et al.*<sup>3</sup> were published in 1970. The molecular formula of pyrazole with the numbering of the atoms is shown in Fig. 1. This

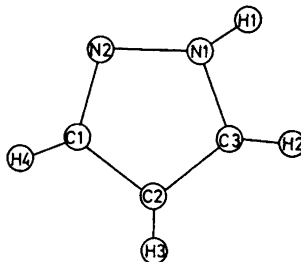


*Fig. 1.* The molecular formula of pyrazole with the numbering of atoms as used in the text.

\* Present address: Texas A & M University, College of Science Department of Chemistry, College Station, 77843 Texas, U.S.A.

X-ray work was carried out for comparing X-ray and neutron diffraction results and for comparing bond lengths obtained by crystal diffraction with those obtained from microwave studies by Nygaard *et al.*<sup>4</sup>

### EXPERIMENTAL

Clear oblong prismatic crystals of pyrazole of analytical grade were formed by sublimation. Five prism faces parallel to the *c*-axis were observed.

Two sets of data, one at 108 K and one at 295 K, were collected using a Buerger-Supper equi-inclination diffractometer automated by a Pace control unit. The crystals used were shaped as cylinders, using a small lathe and a diamond tool. One crystal was ground to a diameter of 0.45 mm and was used for collection of data at room temperature. The length of the crystal exceeded the diameter of the X-ray beam. The crystal used in the low temperature experiment was of diameter 0.25 mm, and it was short enough to be completely bathed in the X-ray beam.

Another room temperature data set was collected using a Picker automatic four-circle diffractometer controlled by a PDP-8 computer. The crystal used in this experiment was nearly cylindrical with a diameter of 0.3 mm and was also completely bathed in the X-ray beam. All crystals were encapsulated in sealed Lindemann glass capillaries. Intensity measurements were carried out using MoK $\alpha$  radiation selected by monochromators designed and built in this department.<sup>5</sup> The counting chain included a scintillation counter and a pulse-height analyzer. The dead-time of the counting chain of the Supper-Pace instrument was determined as 2.7  $\mu$ s using a method described by Chipman.<sup>6</sup> The results are depicted in Fig. 2. Data were obtained from a crystal cooled to 108 K by

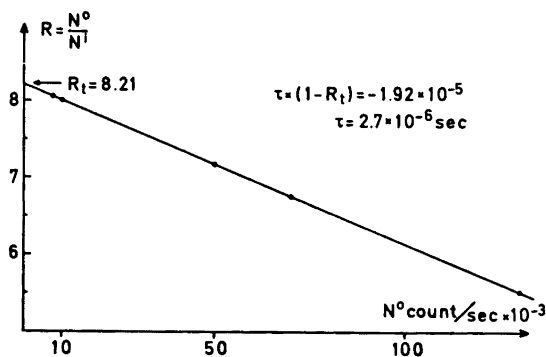


Fig. 2. Absorption coefficient of a zirconium foil measured at various count rates.  $N^0$  is the count rate of the peak of a strong reflection measured without the zirconium foil and  $N^1$  is the count rate of the attenuated reflections.  $N^0$  was varied by measuring different reflections.

blowing a stream of cold nitrogen on to the crystal. A stream of dry nitrogen at room temperature surrounded the cold stream coaxially. Ice formation on the crystal was not completely eliminated but was not large enough to influence the results. A thermo couple (iron-constantan) was placed 3 mm from the crystal. No temperature difference was measurable by moving the thermo couple in a region of 10 mm from this position. The temperature was recorded continuously and showed fluctuations of 2–3°C. Weissenberg and precession photographs of the principal zones were recorded at 108 K as well. The photographs showed no indication of change in space group upon cooling.

At room temperature four symmetry related reflections were measured in general. At 108 K only two symmetry related reflections were recorded. In the Supper-Pace data

collection, a standard reflection was measured every twenty reflections as an internal standard. A best straight line was estimated for the internal standards on each layer line and the reflections were scaled accordingly. The layer lines were scaled together using the 0,10,0 reflection as an overall standard reflection. The strongest reflections were corrected for lost counts in the following way. The integrated intensity is defined as the counting rate integrated over the time of measurement,  $P = \int N(t)dt$ . The corrected counting rate  $N_c$  is related to the observed counting rate  $N$  by the expression  $N_c = N/(1 - \tau N)$  where  $\tau$  is the dead-time of the counting chain. The corrected integrated intensity  $P_c$  is related to the observed intensity by means of the expression  $P_c = P + \tau \int N^2 dt$  to a first order approximation. The integration is performed using the assumption that the intensity distribution  $N(t)$  around the Bragg-position is Gaussian-shaped with a width at half peak height maximum of  $\alpha^\circ$ . The following expression for the corrected integrated intensity is consequently:

$$P_c = P(1 + P \cdot \tau \cdot \text{scanrate} / \alpha \sqrt{2})$$

In the data processing program the widths at half peak height maximum for each reflection were estimated using an experimentally determined relation between  $\alpha$  and  $\sin \theta/\lambda$ . The 1,2,1 reflection in the room temperature set was removed because of the very high correction (25 %); the corrections needed were in all other cases in the range 0–10 %. The intensities from the large crystal were corrected for changes in irradiated volume caused by changes in inclination angles.

Intensities were measured on the Picker diffractometer with the  $\theta - 2\theta$  scan technique. Three standard reflections were measured every 20 reflections thus scaling the previous 20 reflections on the common scale. Averages were taken over symmetry related Lp-corrected reflections, and in general the data showed a good internal consistency. Table 1 summarizes selected characteristics of the three data sets.

Table 1. The first two columns show the number of independent observations before and after removal of reflections where  $F^2 < 3\sigma(F^2)_{\text{count}}$ . Column three gives a measure of the internal consistency of the data.

$$R = \left( \sum_{hkl} (\sum_{\text{symmetry related}} |F^2|) - F^2 \right) / \sum_{hkl} F^2$$

	Number of reflections	Number of significant reflec.	R-value	$\sin \theta_{\text{max}}$	Extinction parameter
Supper Pace 108 K	2051	957	0.054	0.63	
Supper Pace 295 K	2385	852	0.037	0.61	$3.1 \times 10^{-4}$
Picker 295 K	950	535	0.025	0.42	$3.2 \times 10^{-5}$

#### CRYSTAL DATA

The space group is  $P2_1cn$  at both temperatures, and the unit cell dimensions at 108 K are  $a = 8.190 \text{ \AA}$ ,  $b = 12.588 \text{ \AA}$ ,  $c = 6.773 \text{ \AA}$ , while at 295 K  $a = 8.232 \text{ \AA}$ ,  $b = 12.840 \text{ \AA}$ , and  $c = 7.054 \text{ \AA}$ . Linear absorption coefficient for  $\text{MoK}\alpha$  is  $1 \text{ cm}^{-1}$ .

Table 2. Observed and calculated structure factor amplitudes for the low temperature data. The scale is ten times the absolute scale.

Table with 40 columns of numerical data representing structure factor amplitudes. The columns are labeled with Miller indices (h, k, l) and corresponding values. The data is organized in a grid-like format with some columns containing multiple values for a single index.

## REFINEMENT

The three sets of data were refined by the methods of least squares employing a program written by G. S. Pawley. The weights used were  $W = 1/(\mu F)^2$  where  $\mu F = (\sigma(F^2)_{\text{count}} + 1.02 \times F^2)^{1/2} - F$  and  $\sigma(F^2)_{\text{count}}$  is the standard deviation of an observation based on counting statistics. Furthermore a routine for isotropic extinction correction based upon Zachariassen's 1967 paper<sup>8</sup> and used as described by Larson<sup>9</sup> was included in the least squares program. Only the two room temperature data sets were refined with respect to extinction as no indication of extinction effects were found in the low temperature set. The atomic scattering factors used for carbon and nitrogen are those of Cromer and Mann.<sup>10</sup> For hydrogen we used the values given by Stewart *et al.*<sup>11</sup> Constrained refinements were carried out for different models with the three data sets. The constrained refinement procedure described by Pawley<sup>7</sup> was used. Three different models were finally selected as being the more chemically reasonable. In the first model the two crystallographically independent molecules were assumed to be identical and the temperature movements of the atoms were treated as if the molecules moved as rigid bodies (IR). In the second model (INR), the two molecules were assumed to be geometrically identical, but all nitrogen and carbon atoms were allowed independent and anisotropic movements, and the hydrogen atoms were allowed independent and isotropic vibrations. The third model (NINR) was a conventional least squares refinement with nine parameters per heavy atom and four parameters per hydrogen atom. A fourth model could make use of the expected planarity of the molecules. Because of singularity problems in the least squares matrix, it was necessary to keep the *z*-coordinates of the two nitrogen atoms and of one carbon atom fixed with respect to a plane defined by the inertia axis of the molecules. A further constraint to planarity would only decrease the parameter space with two dimensions. This was considered too small a change for making valid statistical conclusions.

Table 2 shows the observed structure factors multiplied by 10 for the low temperature data set together with the calculated structure factors based on the INR model.

## DISCUSSION

Table 3 shows results from the different refinements together with percentage points of the statistical distribution of  $\mathcal{R}$  defined by Hamilton<sup>12</sup> and calculated by the approximation given by Pawley.<sup>13</sup> It is seen that one can reject the hypothesis that the molecules move as rigid bodies for all three sets of data at 0.1 % significance level. The improvements in *R*-values when the constraint of rigid body movement is released is much more pronounced for the room temperature data sets than for the low temperature data set. An important feature in the rigid body constraint is the instability of the least squares system as pointed out by Johnson<sup>14</sup> and Pawley,<sup>15</sup> because the molecules approximate circles in shape. This instability is clearly shown if one makes a Schomaker and Trueblood<sup>16</sup> least squares refinement on the  $u_{ij}$

*Table 3.* Results of refinements on three different models: the two crystallographically independent molecules assumed to be identical in geometry and moving as rigid bodies (IR), the rigid body constraint released (INR) and, finally, a conventional least squares model (NINR). The *R*-factor ratios show a significant improvement for all three sets of data by releasing the rigid body constraint, whereas the improvement obtained by releasing the identity constraint appears to be statistically significant only for the two room-temperature sets of data.

Data set		IR	INR	NINR	$\frac{R_w(\text{IR})}{R_w(\text{INR})}$	$\mathcal{R}_{28,m,0.001}$	$\frac{R_w(\text{INR})}{R_w(\text{NINR})}$	$\mathcal{R}_{21,m,z}$	<i>z</i>
$R_w = [\sum w(F_o - F_c)^2]^{\frac{1}{2}}$	Low temp.	50.892	47.749	47.223	1.066	1.033	1.011	1.012	0.50
	Room temp.	77.910	59.917	58.224	1.300	1.040	1.029	1.028	0.005
	Picker	45.287	33.764	30.116	1.344	1.066	1.121	1.057	0.001
$R_w = [\sum w(F_o - F_c)^2]$	Low temp.	0.065	0.061	0.060	1.066		1.017		
	Room temp.	0.063	0.048	0.047	1.313		1.021		
$\sum w(F_o)^2]^{\frac{1}{2}}$	Picker	0.046	0.034	0.030	1.353		1.133		
Number of parameters	Low temp.	73	101	122					
	Room temp.	74	102	123					
	Picker	74	102	123					

obtained from one of the models refined. If the **U** tensor of the hydrogens is changed from

$$\begin{Bmatrix} .02 & 0 & 0 \\ 0 & .02 & 0 \\ 0 & 0 & .02 \end{Bmatrix} \text{ to } \begin{Bmatrix} .015 & 0 & 0 \\ 0 & .015 & 0 \\ 0 & 0 & .02 \end{Bmatrix}$$

the principal axes of **L** change from (7.90, 3.25, .13)Å<sup>2</sup> to (4.62, 02, -1.38)Å<sup>2</sup>. This is physically impossible.

There is also a statistically significant improvement in *R*-values by removing the identity constraint in the case of the room temperature data sets, whereas for the low temperature data the identity hypothesis cannot be rejected. Although the extra parameters, used in allowing for small differences between the two crystallographically independent molecules, seem to carry a statistical significance, the surroundings of the two molecules differ so little that differences in crystalline fields cannot support an assumption of inequality of the two molecules. Furthermore the surroundings around the molecules are not much different at 108 K where the two molecules seem to be identical.

The apparent disagreement between the physically and chemically plausible results and the statistical indication may be explained as follows. The two sets of atoms in the crystallographically independent molecules are approximately related via a pseudo-two-fold *b*-axis at  $Z = \frac{1}{2}$ . The pseudo-symmetry relation gives rise to large correlation coefficients between related parameters in the conventional least squares refinement where the molecules are treated as being independent entities. Correlation coefficients as large as 0.8 are found, *e.g.* between *x*-parameters of pseudo-symmetry related atoms. The difference in effective number of degrees of freedom between the constrained (identical molecules) and the unconstrained (independent molecules) models is difficult

to define with highly correlated parameters. The  $R$ -ratio test may be seriously affected by departures from the assumed conditions of normally distributed random errors in the observations. Because of the pseudo symmetry, certain classes of reflections like  $0kl$  are systematically weak and are therefore subject to fairly large statistical errors. The  $R$ -ratio test may therefore not be strictly applicable. We propose that the constrained refinements assuming the two crystallographically independent molecules to be geometrically identical lead to the "best" results for the geometry of the pyrazole molecule employing the available data. Since librational corrections are difficult to apply, we propose that the data measured at 108 K lead to a structure in which the bond lengths are less subject to corrections than the structures obtained from the room temperature data.

The crystal structure of pyrazole is described in detail elsewhere (Ehrlich,<sup>1</sup> and Larsen *et al.*<sup>3</sup>). In Tables 4 and 5 are listed coordinates and temperature factors for the two data sets collected on the Supper-Pace diffractometer. It must be remembered by comparing coordinates at the different temperatures that cell edges differ up to 4 %. Figs. 3, 4, and 5 show bond lengths and bond angles for the INR model based on the three data sets. The standard deviations are dubious as they are calculated from marginal standard deviations on the position parameters not taking into account the special problems the constraints impose on the least squares moment matrix. The sum of the angles in the ring indicates that the molecule is planar. A calculation of distances

Table 4. Atomic positions in Å units. Least squares standard deviations are in the range 0.003–0.008 Å for heavy atoms and 0.02 Å for hydrogen atoms.

Molecule 1				Molecule 2		
$x$	$y$	$z$		$x$	$y$	$z$
108 K						
7.0383	1.2357	7.7162	N(1)	1.2755	2.3205	3.3719
7.1500	2.2790	6.8630	N(2)	1.2126	1.2420	2.5584
5.9530	2.3484	6.2911	C(1)	2.4421	0.7410	2.6032
5.0876	1.3805	6.7852	C(2)	3.2683	1.4741	3.4455
5.8269	0.6714	7.6967	C(3)	2.4835	2.4952	3.9164
7.7178	1.0840	8.2990	H(1)	0.5016	2.7491	3.5760
5.6045	–0.0650	8.3974	H(2)	2.6051	3.2289	4.6443
4.1922	1.2855	6.5340	H(3)	4.1590	1.2641	3.6364
5.7683	3.0164	5.7200	H(4)	2.6272	–0.0284	2.1785
295 K						
7.0194	1.2985	8.0661	N(1)	1.2262	2.3854	3.5197
7.1361	2.3028	7.1819	N(2)	1.1581	1.3209	2.7035
5.9568	2.3358	6.5847	C(1)	2.3723	0.8005	2.7619
5.1063	1.3751	7.0631	C(2)	3.2027	1.5132	3.5850
5.8149	0.7251	8.0260	C(3)	2.4343	2.5266	4.0690
7.7190	1.1062	8.5473	H(1)	0.5127	2.8787	3.5937
5.6103	–0.0390	8.5857	H(2)	2.6311	3.2780	4.6484
4.2048	1.2118	6.7650	H(3)	4.1293	1.3208	3.7657
5.8404	2.9822	5.9417	H(4)	2.5172	0.0403	2.2662

Table 5. The anisotropic temperature factors in  $\text{\AA}^2$  scaled by  $10^3$  in the crystal orthogonal coordinate system. Isotropic  $B$ 's for hydrogen have units  $\text{\AA}^2/8\pi^2$ .

Molecule 1						Molecule 2						
$u_{11}$	$u_{22}$	$u_{33}$	$u_{12}$	$u_{13}$	$u_{23}$	108 K	$u_{11}$	$u_{22}$	$u_{33}$	$u_{12}$	$u_{13}$	$u_{23}$
11	14	23	-2	-3	-3	N(1)	15	16	17	4	3	4
11	18	24	0	-3	4	N(2)	13	20	21	-4	-2	-3
19	15	17	4	-2	1	C(1)	18	13	22	-2	-1	0
14	17	25	-6	0	0	C(2)	11	15	14	-4	-5	3
12	12	24	-3	0	0	C(3)	11	16	20	1	1	-3
		0.50				H(1)			0.68			
		3.71				H(2)			2.76			
		1.04				H(3)			0.99			
		3.88				H(4)			0.18			
295 K												
44	56	67	4	-10	-2	N(1)	40	57	63	9	4	3
48	57	73	-7	-3	2	N(2)	43	55	71	-2	-13	2
59	61	55	-3	-7	6	C(1)	52	47	63	3	-3	-2
39	63	66	-6	-10	-8	C(2)	40	62	57	3	-4	2
44	52	70	-3	-1	3	C(3)	45	59	54	-1	-4	-7
		5.28				H(1)			5.42			
		5.82				H(2)			5.08			
		4.69				H(3)			5.79			
		6.16				H(4)			4.65			

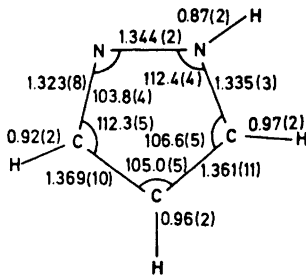


Fig. 3. Geometry of the pyrazole molecule based on the room temperature Supper data set, assuming the two molecules to be identical and non-rigid.

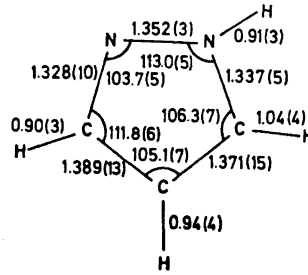


Fig. 4. Geometry of the pyrazole molecule based on the low temperature Supper data set, assuming the two molecules to be identical and non-rigid.

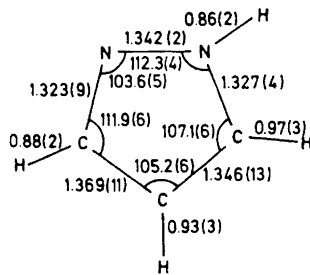


Fig. 5. Geometry of the pyrazole molecule based on the room temperature Picker data set, assuming the two molecules to be identical and non-rigid.

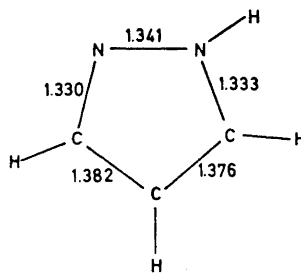


Fig. 6. Geometry of the pyrazole molecule based on the room temperature neutron data. Average over two independent molecules.



of the atoms from the best plane through the heavy atoms gives for the room temperature data sets 0.002 Å on the average, and for the low temperature data set a mean of 0.004 Å. For comparison the geometry of the pyrazole molecule as found by neutron diffraction<sup>3</sup> is shown in Figs. 6 and 7. Fig. 8 describes the molecular geometry which was found using microwave spectroscopy.<sup>4</sup>

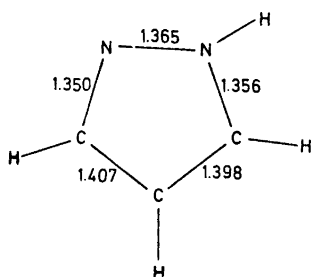


Fig. 7. Geometry of the molecule based on the room temperature neutron data as corrected for rigid body motion. Average over two independent molecules.

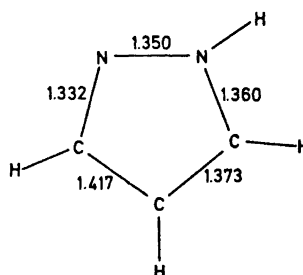


Fig. 8. Microwave substitution structure corrected to equilibrium structure.

In the crystalline state the ring atoms of the pyrazole molecule conform closely to *mm* symmetry. The differences in distances between N(2)–C(1) and N(1)–C(3), and between C(1)–C(2) and C(2)–C(3) are small in all cases. They are, however, systematic. N(2)–C(1) is in all cases found smaller than N(1)–C(3), and C(2)–C(3) is systematically smaller than C(1)–C(2). This is in accordance with the gas phase structure as determined by microwave spectroscopy.<sup>4</sup> Here, however, the differences are more pronounced. The following qualitative explanation is offered. The pyrazole molecule has a pronounced aromatic character. In the free state the unsymmetrical disposition of the hydrogen atoms enforces a certain degree of single bond-double bond alternation upon the distribution of bonding electrons. In the solid state the hydrogen bonding results in a slight redistribution of bonding electrons thus allowing the molecule to assume a more nearly symmetrical configuration.

The spectroscopic and the diffraction results refer to molecules in different vibrational quantum states. In neither case are the distances those of the hypothetical minimum of the potential function. Nevertheless, the experimental evidence appears to be strong enough to lead to the conclusion that the electron redistribution, which takes place upon transfer of a molecule from the gas phase to the crystalline phase, results in experimentally observable changes in bond lengths.

*Acknowledgements.* The Danish State Science Foundation is thanked for providing the Supper-Pace diffractometer. F. Krebs Larsen of this department is thanked for an active interest in this work and for helpful discussion. Rita Grønbaek Hazell and G. Stuart Pawley are thanked for use of their programs and for helpful advice on computing. We are also much indebted to Dr. Lise Nygaard for her communicating the results of the microwave investigation prior to the publication of her results.

## REFERENCES

1. Ehrlich, H. W. W. *Acta Cryst.* **13** (1960) 946.
2. Berthou, J., Elguero, J. and Rérat, C. *Acta Cryst.* **B 26** (1970) 1880.
3. Larsen, F. K., Lehmann, M. S., Sotofte, I. and Rasmussen, S. E. *Acta Chem. Scand.* **24** (1970) 3248.
4. Nygaard, L., Christen, D., Tormod Nielsen, J., Pedersen, E. J., Snerling, O., Vestergaard, E. and Sørensen, G. O. *J. Mol. Struct. To be published.*
5. Rasmussen, S. E. and Henriksen, K. *J. Appl. Cryst.* **3** (1970) 100.
6. Chipman, D. R. *Acta Cryst.* **A 25** (1969) 209.
7. Pawley, G. S. *Advances in Structure Research by Diffraction Methods*, Pergamon London 1972, Vol. 4.
8. Zachariasen, W. H. *Acta Cryst.* **23** (1967) 558.
9. Larson, A. C. *Acta Cryst.* **23** (1967) 664.
10. Cromer, D. T. and Mann, J. B. *Acta Cryst.* **A 24** (1968) 321.
11. Stewart, R. F., Davidson, E. R. and Simpson, W. T. *J. Chem. Phys.* **42** (1965) 3175.
12. Hamilton, W. C. *Acta Cryst.* **18** (1965) 502.
13. Pawley, G. S. *Acta Cryst.* **A 26** (1970) 691.
14. Johnson, C. K. Paper given at the Ottawa Summer School on Crystallographic Computing. Munksgaard, Copenhagen 1970.
15. Pawley, G. S. *Acta Cryst.* **A 26** (1970) 289.
16. Schomaker, V., and Trueblood, K. N. *Acta Cryst.* **B 24** (1968) 63.

Received January 22, 1973.